Dimensionality of $Mn^{II}Cu^{II}$ Bimetallic Compounds and Design of Molecular-Based Magnets

Humberto O. Stumpf,[†,1] Yu Pei,[†] Olivier Kahn,*[,†] Jorunn Sletten,[‡] and Jean Pierre Renard[§]

Contribution from the Laboratoire de Chimie Inorganique, URA No. 420, Université de Paris Sud, 91405 Orsay, France, Department of Chemistry, University of Bergen, 5007 Bergen, Norway, and Institut d'Electronique Fondamentale, URA No. 022, Université de Paris Sud, 91405 Orsay, France

Received December 30, 1992

Abstract: Four compounds have been synthesized, the formulas of which are MnCu(opba)(DMSO)$_3$ (**1**), MnCu(opba)·0.7DMSO (**2**), $(NBu_4)_2Mn_2[Cu(opba)]_3$·6DMSO·$H_2O$ (**3**), and $(NBu_4)_2[Mn_2Cu(opba)]_3$ (**4**), with opba standing for *o*-phenylenebis(oxamato). The crystal structure of **1** has been determined. **1** crystallizes in the monoclinic system, space group $P2_1/n$. The lattice parameters are a = 16.969(7) Å, b = 8.367(1) Å, c = 18.258(7) Å, and Z = 4. The structure consists of well-separated $Mn^{II}Cu^{II}$ zigzag chains. The copper atom is in a square pyramidal environment, and the manganese atom is in an octahedral environment with a *cis* coordination unprecedented for this type of compound. **2** is obtained by heating **1** under vacuum at 140 °C. **3** results from our attempt to cross-link the chains with the $[Cu(opba)]^{2-}$ bisbidentate ligand and, therefore, to increase the dimensionality of the system. **4** is obtained by heating **3** under vacuum at 170 °C. The probable structure of **3** (and **4**) is that of a $Mn^{II}Cu^{II}$ two-dimensional network, in which the manganese atom is surrounded by three Cu(opba) groups instead of two in the chain compound. The magnetic properties of the four compounds have been investigated in a thorough manner. **1** shows the characteristic behavior of a one-dimensional ferrimagnet, with a Mn(II)–Cu(II) interaction parameter J equal to −31.3 cm^{-1} ($H = -J_{MnCu}\sum_i S_{Mn,i}\cdot S_{Cu,i}$). **2** behaves as an amorphous magnet, with a spontaneous magnetization below T_c = 6.5 K. **3** shows an abrupt magnetic transition at T_c = 15 K, with a spontaneous magnetization below T_c. The magnetization versus magnetic field curve for **3** indicates that in the magnetically ordered phase all the manganese local spins are aligned along a direction and the copper local spins along the opposite direction. The saturation magnetization obtained within a field of a few tens of oersteds is 7.1 $N\beta$. Finally, when the DMSO and water molecules of **3** are removed, affording **4**, T_c is shifted to 22 K. The EPR powder spectra of **1**–**4** have also been investigated. The line widths decrease from **1** to **3** and **4**, which suggests that the three-dimensional ordering in **2**–**4** is dominated by the exchange interaction rather than the dipolar effect. The relationship between structures and magnetic properties for compounds **1**–**4** are discussed in detail.

Introduction

At present there is a rapid development within the field of molecular-based magnets. Three international conferences were devoted to this subject in the last three years.[2-4] This situation has been induced by the discovery of the first molecular-based magnets exhibiting a spontaneous magnetization below a critical temperature T_c and by the perspectives offered by this new class of molecular materials, in particular, as active elements of magneto-optical devices.

Let us summarize briefly the state of the art concerning the molecular-based magnets. We will distinguish three types of compounds according to the origin of the unpaired electrons. These types are the following: (i) The unpaired electrons entirely arise from p atomic orbitals. We are then faced with purely organic magnets. Two cases are fully characterized, namely the β phase of *p*-nitrophenyl nitronyl nitroxide with T_c = 0.6 K[5,6] and a dinitronyl nitroxide described quite recently by Rassat and co-workers with T_c = 1.48 K.[7] In the former case, all the interactions are through space; in the latter, there are both through-space and through-bond interactions. A third compound, potentially very interesting, would deserve to be better characterized, namely C_{60}(TDAE) with TDAE standing for tetrakis(dimethylamino)ethylene. T_c would be around 16 K.[8] (ii) Some of the magnetic electrons arise from d and some others from p orbitals. This is the metal–organic radical approach. The magnetic units may be totally separated within the crystal lattice. All the interactions are through space, and T_c is below 8 K.[9-13] Metals and organic radicals may be chemically linked to form chains, and T_c is below 20 K.[14-16] The metal spin carriers may be chemically linked to the organic radicals in a three-dimensional

† Laboratoire de Chimie Inorganique, Université de Paris Sud.
‡ University of Bergen.
§ Institut d'Electronique Fondamentale, Université de Paris Sud.

(1) Permanent address: Departamento de Quimica, Universidade Federal de Minas Gerais, CEP 31270, Belo-Horizonte, MG-Brazil.

(2) *Proceedings of the Symposium on Ferromagnetic and High Spin Molecular Based Materials*; Miller, J. S., Dougherty, D. A., Eds.; Molecular Crystals and Liquid Crystals, No. 176; Gordon & Breach: London, 1989.

(3) Gatteschi, D.; Kahn, O.; Miller, J. S.; Palacio, F. *Magnetic Molecular Materials*; NATO ASI Series; Kluwer: The Netherlands, Dordrecht, 1991.

(4) *Proceedings of the International Symposium on Chemistry and Physics of Molecular Based Magnetic Materials*; Iwamura, H., Itoh, K., Kinoshita, M., Eds.; Molecular Crystals and Liquid Crystals; Gordon & Breach: London, 1993.

(5) Turek, P.; Nozawa, K.; Shiomi, D.; Awaga, K.; Inabe, T.; Maruyama, Y.; Kinoshita, M. *Chem. Phys. Lett.* **1991**, *180*, 327.

(6) Tamura, M.; Nakazawa, Y.; Shiomi, D.; Nozawa, K.; Hosokoshi, Y.; Ishikawa, M.; Takahashi, M.; Kinoshita, M. *Chem. Phys. Lett.* **1991**, *86*, 401.

(7) Chiarelli, R.; Novak, M. A.; Rassat, A.; Tholence, J. L. *Nature* **1993**, *363*, 147.

(8) Allemand, P. M.; Khemani, K. C.; Koch, A.; Wudl, F.; Holczer, K.; Donovan, S.; Grüner, G.; Thompson, J. D. *Science* **1991**, *253*, 301.

(9) Miller, J. S.; Calabrese, J. C.; Rommelmann, H.; Chittipedi, S. R.; Zhang, J. H.; Reiff, W. M.; Epstein, A. J. *J. Am. Chem. Soc.* **1987**, *109*, 769.

(10) Broderick, W. E.; Thomson, J. A.; Day, E. P.; Hoffman, B. M. *Science* **1990**, *249*, 401.

(11) Yee, G. T.; Manriquez, J. M.; Dixon, D. A.; McLean, R. S.; Groski, D. M.; Flippen, R. B.; Naraya, K. S. *Adv. Mater.* **1991**, *3*, 309.

(12) Broderick, W. E.; Hoffman, B. M. *J. Am. Chem. Soc.* **1991**, *113*, 6334.

(13) Eichhorn, D. M.; Skee, D. C.; Broderick, W. E.; Hoffman, B. M. *Inorg. Chem.* **1993**, *32*, 491.

(14) Caneschi, A.; Gatteschi, D.; Renard, J. P.; Rey, P.; Sessoli, R. *Inorg. Chem.* **1989**, *28*, 1976, 3314.

(15) Caneschi, A.; Gatteschi, D.; Sessoli, R.; Rey, P. *Acc. Chem. Res.* **1989**, *22*, 392.

(16) Miller, J. S.; Calabrese, J. C.; McLean, R. S.; Epstein, A. J. *Adv. Mater.* **1992**, *4*, 498.

0002-7863/93/1515-6738$04.00/0

network. T_c may then be very high. This is probably what happens in $V(TCNE)_2 \cdot xCH_2Cl_2$, with T_c above 300 K.[17] (iii) All the magnetic electrons arise from d orbitals. Again T_c is expected to be higher as the through-bond/through-space interaction becomes more predominant. T_c is of the order of 1 K or less if the magnetic units only interact through space.[18] T_c is below 10 K when the structure consists of well-separated chains[19] and may reach 30 K when the chains are brought closer to each other as a result of thermal treatment.[20,21] For oxalato-bridged compounds of higher dimensionality, the structure of which is still unknown, T_c is in the 5–15 K temperature range.[22]

From what precedes, it emerges that, irrespective of the nature of the spin carriers, T_c directly depends on the dimensionality. This statement is obvious and at the same time rather disconcerting. It is obvious because the magnetic ordering is most generally a three-dimensional phenomenon. It may exceptionally occur in two dimensions in the case of uniaxial magnetic anisotropy. In no case may it occur in one dimension. Our statement is rather disconcerting because, when the dimensionality increases, some specificities of the molecular chemistry like solubility, processability, or even transparency tend to disappear, and the originality of the molecular-based magnets, as compared to the classical insulating magnets like Fe_3O_4, may then vanish.

Our strategy in designing molecular-based magnets is to assemble $Mn^{II}Cu^{II}$ molecular units or chains within the crystal lattice in such a way that the Cu(II) ion of a unit or a chain preferably interacts with the Mn(II) ion of the neighboring unit or chain.[23] We are also trying to increase the dimensionality of the compounds and at the same time to retain the molecular character. We report the latest results along this line in this paper. We will describe four compounds resulting from the reaction of the Mn(II) ion with the Cu(II) precursor $[Cu(opba)]^{2-}$

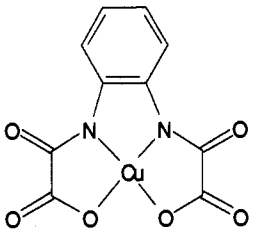

where opba stands for *o*-phenylenebis(oxamato). The first compound, of formula $MnCu(opba)(DMSO)_3$ (**1**), has an unexpected zigzag chain structure. The magnetic study reveals that the chains are almost perfectly isolated within the crystal lattice. Heating **1** at 140 °C under vacuum affords a new compound (**2**) which behaves as an amorphous molecular-based magnet with T_c = 6.5 K. Our attempts to increase the dimensionality led us to a compound of formula $(NBu_4)_2Mn_2[Cu(opba)]_3 \cdot 6DMSO \cdot H_2O$ (**3**) exhibiting a spontaneous magnetization below T_c = 15 K. The DMSO and water molecules of **3** can be removed by a thermal treatment. T_c is then shifted to 22 K. The paper is organized as follows: First, we describe the syntheses of the Cu(II) precursor and of compounds **1–4**. Then, we study in a thorough manner the magnetic susceptibility, the magnetization, and the EPR properties of the compounds. Finally, we discuss the relationships between structure and properties for this class of compound.

(17) Manriquez, J. M.; Yee, G. T.; McLean, R. S.; Epstein, A. J.; Liller, J. S. *Science* **1991**, *252*, 1415.
(18) See, for instance: Carlin, R. L. *Comments Inorg. Chem.* **1991**, *11*, 215.
(19) Kahn, O.; Pei, Y.; Verdaguer, M.; Renard, J. P.; Sletten, J. *J. Am. Chem. Soc.* **1988**, *110*, 782.
(20) Nakatani, K.; Bergerat, P.; Codjovi, E.; Mathonière, C.; Pei, Y.; Kahn, O. *Inorg. Chem.* **1991**, *30*, 3977.
(21) Nakatani, K.; Carriat, P. Y.; Journaux, Y.; Kahn, O.; Lloret, F.; Renard, J. P.; Pei, Y.; Sletten, J.; Verdaguer, M. *J. Am. Chem. Soc.* **1989**, *111*, 5739.
(22) Tamaki, H.; Zhong, Z. J.; Matsumoto, N.; Kida, S.; Koikawa, M.; Achiwa, N.; Hashimoto, Y.; Okawa, H. *J. Am. Chem. Soc.* **1992**, *114*, 6974.
(23) Pei, Y.; Kahn, O.; Nakatani, K.; Codjovi, E.; Mathonière, C.; Sletten, J. *J. Am. Chem. Soc.* **1991**, *113*, 6558.

Experimental Section

Syntheses. The diethyl ester Et_2H_2opba of the *o*-phenylenebis(oxamic acid) was obtained by adding dropwise 7 mL (8.4 g, 0.06 mol) of ethoxalyl chloride to a solution of 3.3 g (0.03 mol) of *o*-phenylenediamine dissolved in 150 mL of THF. The resulting mixture was refluxed for $^1/_2$ h and then filtered to eliminate the solid residue. The THF solution was evaporated, which afforded an oil residue. Slow addition of water resulted in the formation of a white polycrystalline powder which was collected by filtration, washed with water, and dried under vacuum. Yield: 8.6 g (93%). Anal. Calcd for $C_{14}H_{16}N_2O_6$: C, 54.54; H, 5.19; N, 9.09; O, 31.14. Found: C, 54.60; H, 5.17; N, 8.97; O, 30.93.

The copper(II) precursor salt $Na_2[Cu(opba)] \cdot 3H_2O$ was synthesized as follows: Fifty milliliters of an aqueous solution containing 2.52 g (0.063 mol) of NaOH was added to a suspension of 4.62 g (0.015 mol) of Et_2H_2opba in 100 mL of a 9/1 mixture of water/ethanol. The mixture was heated at 70 °C for $^1/_2$ h. Fifty milliliters of an aqueous solution containing 3.62 g (0.015 mol) of $Cu(NO_3)_2 \cdot 3H_2O$ was then added slowly under stirring. The deep-violet solution was filtered and then allowed to evaporate slowly. The polycrystalline precipitate was collected by filtration, washed with ethanol, and dried. Yield: 5.2 g (85%). Anal. Calcd for $C_{10}H_{10}N_2O_9CuNa_2$: C, 29.17; H, 2.43; N, 6.80; Cu, 15.43; Na, 11.17. Found: C, 29.26; H, 2.45; N, 6.71; Cu, 15.28; Na, 11.20.

The tetra-*n*-butylammonium salt $(NBu_4)_2[Cu(opba)]$ was prepared by adding 90 mL (0.137 mol) of NBu_4OH (40% in water) to a suspension of 10 g (0.0325 mol) of Et_2H_2opba in 250 mL of a 4/1 water/ethanol mixture. The resulting mixture was stirred at 60 °C for 20 min. Fifty milliliters of an aqueous solution containing 5.54 g (0.0325 mol) of $CuCl_2 \cdot 2H_2O$ was then added slowly under stirring. The deep-blue solution was filtered, reduced to 100 mL, and extracted with 400 mL of CH_2Cl_2. The organic phase was separated from the mixture, washed with water until a negative test with $AgNO_3$ was obtained, and dried over Na_2SO_4. The deep-purple solution was allowed to evaporate, and the product that formed (which may be either an oil or a solid) was recrystallized from CH_3CN. Yield: 23.3 g (90%). Anal. Calcd for $C_{42}H_{76}N_4O_6Cu$: C, 63.32; H, 9.54; N, 7.03; O, 12.05; Cu, 7.98. Found: C, 62.99; H, 9.52; N, 7.23; O, 12.06; Cu, 7.89.

$MnCu(opba)(DMSO)_3$ (**1**) was prepared by adding 2.7 g (0.011 mol) of $Mn(CH_3COO)_2 \cdot 4H_2O$ to a solution of 4.1 g (0.01 mol) of $Na_2[Cu(opba)] \cdot 3H_2O$ in 50 mL of dimethyl sulfoxide (DMSO) under stirring at 50 °C. The stirring and the heating were maintained for 15 min, and the resulting blue solution was allowed to stand for 48 h at room temperature. Well-shaped blue crystals then formed; they were collected by filtration, washed with DMSO, and dried under vacuum. Yield: 5.4 g (90%). Anal. Calcd for $C_{16}H_{22}N_2O_9S_3CuMn$: C, 31.97; H, 3.66; N, 4.66; O, 23.95; S, 16.01; Cu, 10.57; Mn, 9.14. Found: C, 31.91; H, 3.62; N, 4.65; O, 23.94; S, 15.93; Cu, 10.28; Mn, 8.94.

The thermal treatment applied to $MnCu(opba)(DMSO)_3$ and affording **2** consisted of warming this compound under vacuum for 4 h around 140 °C. The chemical analysis leads to the formula $MnCu(opba) \cdot 0.7DMSO$. Anal. Calcd for $C_{11}H_{8.2}N_2O_{6.7}S_{0.7}CuMn$: C, 32.50; H, 1.95; N, 6.65; S, 5.33; Cu, 14.82; Mn, 12.82. Found: C, 31.62; H, 2.16; N, 6.46; S, 5.12; Cu, 14.75; Mn, 12.68.

$(NBu_4)_2Mn_2[Cu(opba)]_3 \cdot 6DMSO \cdot H_2O$ (**3**) was synthesized by adding 0.61 g (2.5×10^{-3} mol) of $Mn(CH_3COO)_2 \cdot 4H_2O$ to a solution of 3.2 g (4×10^{-3} mol) of $(NBu_4)_2[Cu(opba)]$ dissolved in 20 mL of DMSO under stirring at 50 °C. The stirring was maintained for 15 min, and then the resulting blue solution was allowed to stand at 30 °C for 3 days. The well-shaped small crystals obtained were collected by filtration, washed with DMSO, and dried under vacuum in a desiccator. Yield: 2.21 g (88%). Anal. Calcd for $C_{74}H_{122}N_8O_{25}S_6Cu_3Mn_2$: C, 44.07; H, 6.05; N, 5.56; S, 9.54; Cu, 9.45; Mn, 5.45. Found: C, 43.85; H, 5.91; N, 5.55; S, 9.55; Cu, 9.87; Mn, 5.39.

$(NBu_4)_2Mn_2[Cu(opba)]_3$ (**4**) was obtained by heating **3** under vacuum at 170 °C for about 4 h. Anal. Calcd for $C_{62}H_{84}N_8O_{18}Cu_3Mn_2$: C, 48.68; H, 5.49; N, 7.32; Cu, 12.46; Mn, 7.18. Found: C, 48.65; H, 5.48; N, 7.32; Cu, 12.50; Mn, 7.06. One will note that the chemical analysis is excellent, confirming that all the DMSO and water molecules have been removed and that the skeleton with the metal sites and bridges has not been affected by the thermal treatment.

X-ray Data Collection and Structure Determination. Diffraction data were collected at 294 K with an Enraf-Nonius CAD-4 diffractometer

Table I. Bond Distances (Å) Involving Non-Hydrogen Atoms in $MnCu(opba)(DMSO)_3$ (1)[a]

Cu–O3	1.964(3)	S3–C15	1.791(6)
Cu–O4	1.985(3)	S3–C16	1.683(7)
Cu–O9	2.305(3)	O1–C2	1.263(5)
Cu–N1	1.909(3)	O2–C1	1.239(5)
Cu–N2	1.912(3)	O3–C1	1.269(5)
Mn–O1	2.164(3)	O4–C10	1.263(5)
Mn–O2	2.224(3)	O5–C9	1.255(5)
Mn–O5[1]	2.201(3)	O6–C10	1.247(5)
Mn–O6[2]	2.195(3)	N1–C2	1.317(5)
Mn–O7	2.131(3)	N1–C3	1.398(5)
Mn–O8	2.147(3)	N2–C4	1.393(5)
S1–O7	1.502(3)	N2–C9	1.305(5)
S1–C11	1.819(5)	C1–C2	1.531(6)
S1–C12	1.793(5)	C3–C4	1.401(5)
S3A–O8	1.494(4)	C3–C8	1.381(6)
S2A–C13	1.808(5)	C4–C5	1.389(6)
S2A–C14	1.783(6)	C5–C6	1.364(6)
S2B–O8	1.45(1)	C6–C7	1.396(6)
S2B–C13	1.75(1)	C7–C8	1.384(6)
S2B–C14	1.67(1)	C9–C10	1.552(6)
S3–O9	1.480(3)		

[a] Superscripts 1 and 2 refer to symmetry operations $^1/_2 + x, ^1/_2 - y, ^1/_2 + z$ and $-^1/_2 + x, ^1/_2 - y, -^1/_2 + z$, respectively.

using graphite-monochromated Mo Kα radiation (λ = 0.710 73 Å). Cell parameters were determined from 24 reflections with 2θ angles between 24 and 38°. The compound crystallizes in the monoclinic system, space group $P2_1/n$. Crystal parameters and refinement results are summarized in Table SI (supplementary material). To avoid solvent loss the crystal was embedded in a thin film of glue. A total of 3352 unique reflections were recorded in the range $2° < 2\theta < 46°$. The intensity of three reference reflections monitored throughout the data collection decreased by 19% on average, and the data were scaled accordingly. The usual corrections for Lorentz and polarization effects were carried out.

The structure was solved by direct methods and refined by the full-matrix least-squares method. Hydrogen atoms belonging to the phenyl group were localized in a difference Fourier map and included in the refinement; the remaining hydrogen atoms were not found. The difference map also revealed disorder in one of the DMSO molecules. A disorder model involving two positions for the sulfur atom was used, the occupation factors converging at 0.83 and 0.17 for S2A and S2B, respectively. After isotropic refinement, an empirical absorption correction was performed.[24] In the final least-squares cycles, all non-hydrogen atoms were refined anisotropically and all hydrogen atoms isotropically, and an extinction parameter was fitted. The highest residual peaks in the difference electron density map are located close to the disordered DMSO molecule. The refinement, minimizing $\sum[w(F_o - F_c)^2]$ and including 2543 reflections with $I > 2\sigma(I)$, converged at $R = 0.053$, $R_w = 0.054$, and $s = 2.56$. All calculations were carried out on a MICRO-VAX II computer with the Enraf-Nonius structure determination programs.[25] The scattering curves, with anomalous dispersion terms included, were those of Cromer and Mann.[26]

Coordinates and isotropic equivalent displacement parameters are listed in Table SII (supplementary material); bond lengths and angles of non-hydrogen atoms, in Tables I and II. Anisotropic thermal parameters, distances and angles involving hydrogen atoms, least-squares planes, and structure factors are listed in Tables SIII–SVI (supplementary material).

Magnetic Measurements. These were carried out with three instruments, namely a Faraday-type magnetometer working in the 4–300 K temperature range, a low-field SQUID magnetometer working below 30 K with magnetic fields on the order of 1 Oe, and a high-field SQUID magnetometer working with magnetic fields up to 80 KOe. The two SQUID instruments can be used down to 1.7 K.

EPR Measurements. The X-band powder EPR spectra were recorded at various temperatures between 4.2 and 300 K with an ER 200D Bruker spectrometer, equipped with a helium continuous-flow cryostat and a Hall probe.

(24) Walker, N.; Stuart, D. *Acta Crystallogr., Sect. A* **1983**, *39*, 158.
(25) Frez, B. A. *The SPD User's Guide (SPDVAX V.3)*; Enraf-Nonius: Deft, The Netherlands, 1985.
(26) Cromer, D. T.; Waber, J. T. *International Tables for X-ray Crystallography*; Kynoch Press: Birmingham, U.K., 1974; Vol IV, p 99 (Table 2.2B).

Table II. Bond Angles (degrees) Involving Non-Hydrogen Atoms in $MnCu(opba)(DMSO)_3$ (1)[a]

O3–Cu–O4	106.3(1)	Mn–O2–C1	112.8(3)
O3–Cu–O9	98.0(1)	Cu–O3–C1	111.1(3)
O3–Cu–N1	84.5(1)	Cu–O4–C10	110.6(3)
O3–Cu–N2	162.2(1)	Mn^2–O5–C9	113.9(3)
O4–Cu–O9	94.1(1)	Mn^2–O6–C10	115.0(3)
O4–Cu–N1	163.9(1)	Mn–O7–S1	145.1(2)
O4–Cu–N2	84.3(1)	Mn–O8–S2A	133.3(2)
O9–Cu–N1	96.2(1)	Mn–O8–S2B	139.0(5)
O9–Cu–N2	95.4(1)	Cu–O9–S3	126.2(2)
N1–Cu–N2	82.4(1)	Cu–N1–C2	114.7(3)
O1–Mn–O2	76.0(1)	Cu–N1–C3	114.6(3)
O1–Mn–O5[1]	97.9(1)	C2–N1–C3	130.7(4)
O1–Mn–O6[1]	162.9(1)	Cu–N2–C4	115.2(3)
O1–Mn–O7	91.2(1)	Cu–N2–C9	115.1(3)
O1–Mn–O8	96.5(1)	C4–N2–C9	129.2(3)
O2–Mn–O5[1]	97.6(1)	O2–C1–O3	125.9(4)
O2–Mn–O6[1]	88.8(1)	O2–C1–C2	116.3(4)
O2–Mn–O7	164.7(1)	O3–C1–C2	117.9(4)
O2–Mn–O8	85.6(1)	O1–C2–N1	129.3(4)
O5[1]–Mn–O6[1]	76.1(1)	O1–C2–C1	119.5(4)
O5[1]–Mn–O7	92.5(1)	N1–C2–C1	111.2(4)
O5[1]–Mn–O8	165.6(1)	N1–C3–C4	114.0(4)
O6[1]–Mn–O7	104.9(1)	N1–C3–C8	126.5(4)
O6[1]–Mn–O8	90.0(1)	C4–C3–C8	119.5(4)
O7–Mn–O8	87.5(1)	N2–C4–C3	113.1(3)
O7–S1–C11	106.8(2)	N2–C4–C5	126.8(4)
O7–S1–C12	105.4(3)	C3–C4–C5	120.0(4)
C11–S1–C12	96.5(3)	C4–C5–C6	119.2(4)
O8–S2A–C13	104.3(3)	C5–C6–C7	122.1(5)
O8–S2A–C14	107.1(3)	C6–C7–C8	118.2(5)
C13–S2A–C14	100.0(3)	C3–C8–C7	121.0(4)
O8–S2B–C13	109.7(8)	O5–C9–N2	130.7(4)
O8–S2B–C14	115.7(7)	O5–C9–C10	118.1(4)
C13–S2B–C14	107.1(7)	N2–C9–C10	111.1(4)
O9–S3–C15	107.0(3)	O4–C10–O6	125.2(4)
O9–S3–C16	107.1(4)	O4–C10–C9	117.9(4)
C15–S3–C16	98.1(4)	O6–C10–C9	117.0(4)
Mn–O1–C2	112.6(3)		

[a] Superscripts 1 and 2 refer to symmetry operations $^1/_2 + x, ^1/_2 - y, ^1/_2 + z$ and $-^1/_2 + x, ^1/_2 - y, -^1/_2 + z$, respectively.

Description of the Structure of $MnCu(opba)(DMSO)_3$ (1)

The structure of $MnCu(opba)(DMSO)_3$ consists of ordered bimetallic chains running in a zigzag fashion along the *n*-glide direction. A section of such a chain is shown in Figure 1 along with the atom-labeling scheme. The copper atom has approximately square pyramidal surroundings with two nitrogen and two oxygen atoms from the opba group in the basal plane and a DMSO oxygen atom in the apical position. The basal Cu–O bond lengths are equal to 1.964(3) and 1.985(3) Å, and the Cu–N bond lengths, to 1.909(3) and 1.912(3) Å, while the apical Cu–O bond length is equal to 2.305(3) Å. The copper atom is displaced by 0.20 Å from a least-squares plane defined by O3, O4, N1, N2 toward the apical position. The dihedral angles between the basal plane of copper and those of the coordinated oxamato groups are equal to 4 and 0°, respectively.

The manganese atom has somewhat distorted octahedral surroundings: two DMSO molecules coordinate in *cis* positions (Mn–O = 2.131(3) and 2.147(3) Å), the other positions being occupied by oxygen atoms from two opba ligands with Mn–O bond lengths ranging from 2.164(3) to 2.224(3) Å. As a consequence of the *cis* coordination of the DMSO molecules, the dihedral angle between the planes of the oxamato groups bonded to manganese is equal to 109.9°.

The separations between neighboring metal atoms within the chain are Mn···Cu = 5.394(1) and 5.442(1) Å across oxamato groups O1, O2, O3, N1, C1, C2 and O4, O5, O6, N2, C9, C10, respectively. Owing to the bulkiness of the DMSO molecules bonded to the metal centers, the chains are very separated from each other. The shortest interchain metal···metal separations are Mn···Mn($1 - x$, $1 - y$, $1 - z$) = 7.209(2) Å and Cu···Mn(x,

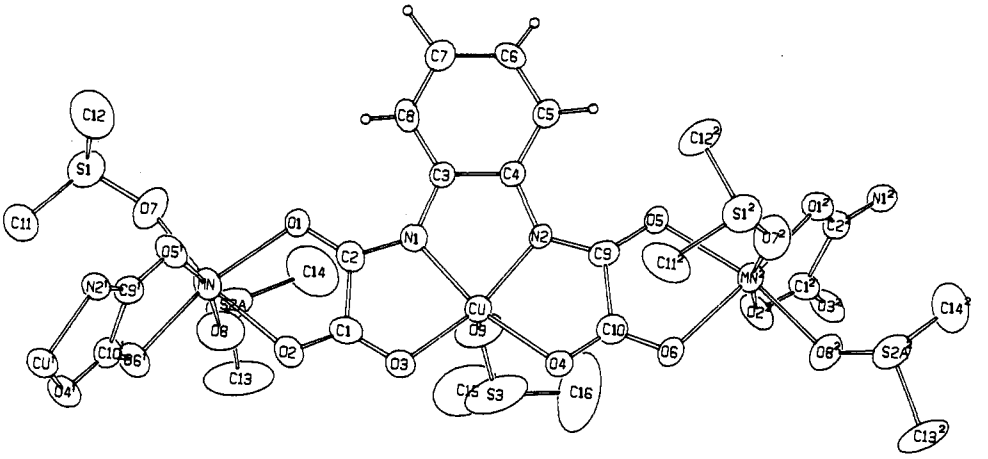

Figure 1. Section of the bimetallic chain in MnCu(opba)(DMSO)$_3$ (**1**). The thermal ellipsoids are plotted at the 50% probability level. Superscripts 1 and 2 denote symmetry operations $^1/_2 + x$, $^1/_2 - y$, $^1/_2 + z$ and $-^1/_2 + x$, $^1/_2 - y$, $-^1/_2 + z$, respectively.

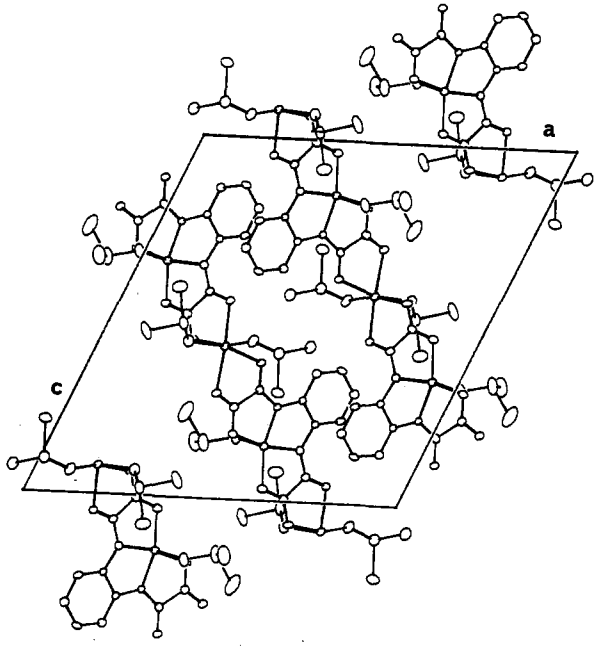

Figure 2. Crystal packing in MnCu(opba)(DMSO)$_3$ (**1**) as viewed down the *b* axis. The origin of the unit cell is in the upper left-hand corner, the *a* axis running horizontally.

$y - 1, z) = 7.505(1)$ Å. The arrangement of neighboring chains is depicted in Figure 2. The planes of the aromatic rings in neighboring chains are also oriented in a zigzag fashion, the dihedral angle being equal to 109°. The shortest C···C separation between two adjacent rings is equal to 3.57 Å.

Magnetic Properties

For the four compounds **1–4**, we studied the temperature dependence of the magnetic susceptibility and the field dependence of the magnetization.

MnCu(opba)(DMSO)$_3$ (1). The temperature dependence of the magnetic susceptibility for MnCu(opba)(DMSO)$_3$ is shown in Figure 3 in the form of the $\chi_M T$ versus T plot, χ_M being the molar magnetic susceptibility and T the temperature. At room temperature $\chi_M T$ equals 4.14 cm^3 K mol^{-1}, which is slightly below what would be anticipated for uncoupled Mn(II) and Cu(II) ions, decreases slowly as T is lowered, exhibits a rounded minimum around 130 K with $\chi_M T = 3.93$ cm^3 K mol^{-1}, then increases more and more rapidly as T is lowered further, and reaches 66.5 cm^3 K mol^{-1} at 1.7 K, the lowest temperature we have investigated. This behavior is characteristic of the one-dimensional ferrimagnetism. At high temperature $\chi_M T$ tends toward the paramagnetic limit; the decrease of χ_{MT} as T is lowered corresponds to a very short range order where the local spins S_{Mn} and S_{Cu} of adjacent metal ions are antiparallel, but without correlation between the MnCu neighboring units. As T is lowered further below the temperature of the minimum of $\chi_M T$, the correlation length within the chain increases, leading in principle to a ferrimagnetic order at absolute zero in the absence of interchain interaction. In the low-temperature range, the magnetic behavior is qualitatively equivalent to what happens for a chain of $S_{Mn} - S_{Cu} = 2$ spins ferromagnetically coupled.[27,28]

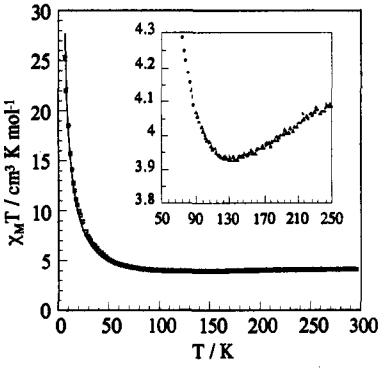

Figure 3. Observed (□) and calculated (—) $\chi_M T$ versus T plots for MnCu(opba)(DMSO)$_3$ (**1**). The data below 30 K were measured at a magnetic field of 1 Oe.

The magnetic susceptibility data may be quantitatively interpreted with a one-dimensional model we described elsewhere[29,30] in which the susceptibility is deduced from a spin Hamiltonian of the form

$$H = -J_{MnCu}\sum_{i=1}^{n} S_{Mn,i}\cdot S_{Cu,i}$$

The summation runs over the n MnCu units along the chain. J_{MnCu} is the interaction parameter between adjacent spin carriers. $S_{Mn} = {}^5/_2$ is treated as a classical spin and $S_{Cu} = {}^1/_2$ as a quantum spin. The parameters of this model in addition to J_{MnCu} are the local Zeeman factors g_{Mn} and g_{Cu}, assumed to be isotropic. The least-squares fitting of the experimental data with this model leads to $J_{MnCu} = -31.3$ cm^{-1}, $g_{Mn} = 1.98$, and $g_{Cu} = 2.10$. The agreement factor defined as $\sum[(\chi_M T)^{calc} - (\chi_M T)^{obs}]^2/[(\chi_M T)^{obs}]^2$

(27) Kahn, O. *Struct. Bonding (Berlin)* **1987**, *68*, 89.
(28) Kahn, O. *Molecular Magnetism*; Verlag-Chemie: New York, in press.
(29) Georges, R.; Curely, J.; Gianduzzo, J. C.; Xu, Q.; Kahn, O.; Pei, Y. *Physica B+C* **1988**, *153*, 77.
(30) Kahn, O.; Pei, Y.; Nakatani, K.; Journaux, Y.; Sletten, J. *New J. Chem.* **1992**, *16*, 269.

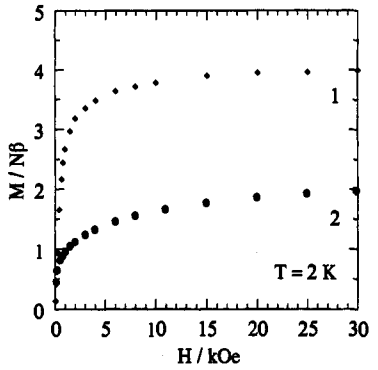

Figure 4. M versus H plot for MnCu(opba)(DMSO)$_3$ (**1**) (♦) and the compound obtained after thermal treatment (**2**) (●) at 2 K.

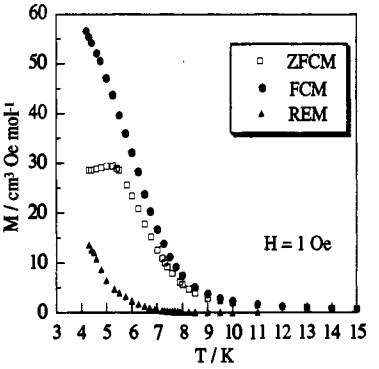

Figure 5. Magnetization M versus T curves for **2**.

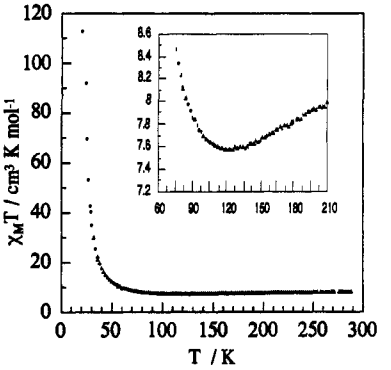

Figure 6. $\chi_M T$ versus T plot for $(NBu_4)_2Mn_2[Cu(opba)]_3 \cdot 6DMSO \cdot H_2O$ (**3**).

is then equal to 2×10^{-4} for 162 experimental points. The theoretical curve closely reproduces the experimental one down to ca. 5 K and then passes slightly above the experimental points, which suggests that extremely weak intermolecular antiferromagnetic interactions superimpose on the dominant intrachain interaction characterized by J_{MnCu}. We have written "suggests" instead of "indicates" because the weakly pronounced difference between observed and calculated $\chi_M T$ values below 5 K might be due also to the inadequacy of our classical—quantum—model in this temperature range. The important point is that the magnetic properties of **1** very closely follow the one-dimensional model. In all the $Mn^{II}Cu^{II}$ chains studied so far,[19-21,31] the interchain interactions provoke a three-dimensional magnetic ordering in the 2.3–14 K temperature range. It is remarkable that there is no indication of three-dimensional magnetic ordering for MnCu(opba)(DMSO)$_3$ down to 1.7 K. This is obviously due to the fact that the bulky DMSO molecules efficiently isolate the chains from each other.

We also investigated the field dependence of the magnetization M up to 80 kOe at 2 K. The curve in the 0–30 kOe field range is shown in Figure 4. As the field H increases, M increases linearly up to 2 kOe, the slope of the curve being in agreement with the magnetic susceptibility at 1 Oe measured independently, and then saturates rapidly. Fifty percent of the saturation magnetization is obtained within 0.4 kOe and 75% within 1.4 kOe. Owing to the negligibly small interchain interactions, a weak field is sufficient to align parallel the $n(S_{Mn} - S_{Cu})$ chain spins. The value of the saturation magnetization, $M_S = 4N\beta$, corresponds exactly to what is expected for all S_{Mn} local spins aligned along the field direction and all the S_{Cu} local spins along the opposite direction. In other respects, the field dependence of the magnetization does not show any sign of intrachain spin decoupling, due to the large value of $|J_{MnCu}|$.

Compound after Thermal Treatment (2). The magnetic properties of the compound after thermal treatment were investigated in the low-temperature range, i.e. below 30 K. The magnetization versus temperature curves at a field of 1 Oe are shown in Figure 5. The field-cooled magnetization (FCM) measured upon cooling down within the field shows a rapid increase of M with a change of sign for the second derivative $\partial^2 M/\partial T^2$ at 6.5 K. The zero-field-cooled magnetization (ZFCM) measured upon cooling down in zero field and then warming up within the field presents a maximum at 6 K. Finally, when the sample is cooled down in zero field and then warmed up in zero field, a remnant magnetization (REM) is observed, which vanishes at 6.5 K. These data indicate that the material behaves as a magnet with a spontaneous magnetization below 6.5 K.

The magnetization versus magnetic field curve at 2 K provides intereting insights into the nature of this new molecular-based magnet. This curve is represented in Figure 4. The value of the slope $(\partial M/\partial H)_{H=0}$ is high, namely 50 cm^3 mol^{-1}, which is perfectly in line with the fact that we are below T_c. As expected, this slope decreases as the field H increases, and the magnetization tends to saturate. Even at 80 kOe, however, the magnetization value is only 2.1 $N\beta$, i.e. roughly half of the saturation magnetization for the precursor **1**. The removal of the DMSO molecules is expected to bring the chains closer to each other. These chains, however, are most probably randomly oriented. The compound is amorphous. As the field increases, the resulting spins of the chains do not align along the field direction any longer but remain canted.

$(NBu_4)_2Mn_2[Cu(opba)]_3 \cdot 6DMSO \cdot H_2O$ (3). The $\chi_M T$ versus T plot for **3** shown in Figure 6 presents a minimum around 120 K, which is characteristic of a ferrimagnetic behavior with Mn(II)–Cu(II) antiferromagnetic interactions and noncompensation of the local spins in the ground state. The $\chi_M T$ value at room temperature, 8.30 cm^3 K mol^{-1}, is already lower than expected for two Mn(II) and three Cu(II) isolated ions. At 120 K, $\chi_M T$ is equal to 7.57 cm^3 K mol^{-1}. As the temperature is lowered below 120 K, $\chi_M T$ increases more and more rapidly and reaches extremely high values before becoming strongly field dependent around 15 K. Such a behavior strongly suggests that the compound orders magnetically with a spontaneous magnetization. This is unambiguously confirmed by the magnetization versus temperature curves within a field of 1 Oe given in Figure 7. The FCM curve displays an abrupt break at 15 K. At any temperature below 15 K the ZFCM is much lower than the FCM, due to the fact that in this temperature range the domain walls do not move freely. The ZFCM curve exhibits a maximum just below 15 K.[32] Finally, the REM vanishes at T_c = 15 K. The magnetization versus magnetic field curve at 5 K is shown in Figure 8. This curve is typical of an almost ideal magnet. The saturation magnetization value, 7.1 $N\beta$, nicely agrees with what is expected for all the S_{Mn} local spins aligned along the field direction and the S_{Cu} local spins along the opposite direction. Around 80% of the saturation is reached within a field of a few tens of oersteds.

(31) Pei, Y.; Verdaguer, M.; Kahn, O.; Sletten, J.; Renard, J. P. *Inorg. Chem.* **1987**, *26*, 138.

(32) Hitzfeld, M.; Ziemann, P.; Buckel, W.; Claus, H. *Phys. Rev. B* **1984**, *29*, 5023.

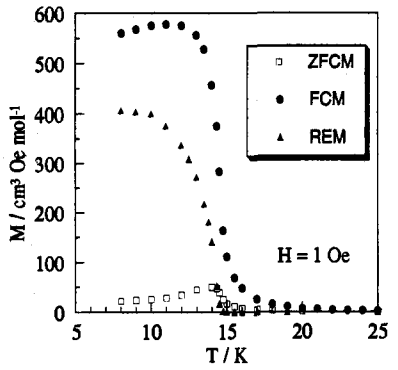

Figure 7. Magnetization M versus T curves for $(NBu_4)_2Mn_2[Cu(opba)]_3 \cdot 6DMSO \cdot H_2O$ (**3**).

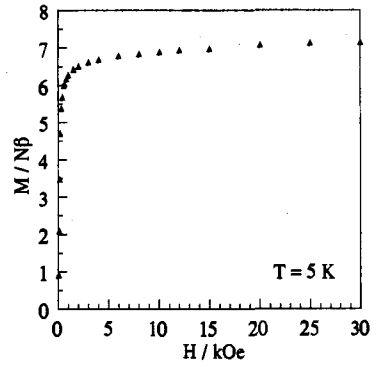

Figure 8. M versus H plot for $(NBu_4)_2Mn_2[Cu(opba)]_3 \cdot 6DMSO \cdot H_2O$ (**3**) at 5 K.

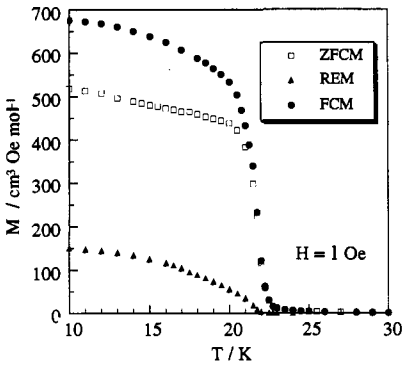

Figure 9. Magnetization M versus T curves for $(NBu_4)_2Mn_2[Cu(opba)]_3$ (**4**).

$(NBu_4)_2Mn_2[Cu(opba)]_3$ (4). The magnetic behavior of **4** is rather similar to that of **3**, except that the critical temperature is shifted to $T_c = 22$ K, as shown in Figure 9. One will note that the REM is weaker for **4** than for **3**. This REM is not an intrinsic quantity but depends on various factors like the grain size and shape within the sample.

EPR Spectra

The powder EPR spectra for the four compounds **1–4** each exhibit a single and almost symmetrical band centered at $g = 2.00$, without detectable half-field transition. The line widths, however, are very different. At room temperature they are 160 Oe for **1**, 100 Oe for**2**, and 70 Oe for both **3** and **4** and do not vary significantly with temperature. It is now well established that the line widths of magnetically concentrated systems result from two opposite effects, namely the dipolar interactions which broaden the lines and the exchange interactions which narrow the lines.[33] In the present case, the exchange interaction effect clearly dominates. The thermal treatment applied to **1** where the chains are almost perfectly isolated results in an amorphous magnet **2** ($T_c = 6.5$ K), with a large decrease of the EPR line width. The weaker line widths are obtained with **3** and **4**, which behave as almost ideal magnets below $T_c = 15$ and 22 K, respectively. The same evolution was observed in the other Mn^{II}-Cu^{II} chain compounds studied so far. For instance, the line width is 327 Oe for $MnCu(obbz) \cdot 5H_2O$, which has a very strong one-dimensional character, and 104 Oe for $MnCu(obbz) \cdot H_2O$, showing a ferromagnetic transition at $T_c = 14$ K.[20]

Discussion

In this section we discuss the relationships between structure and properties for compounds **1–4**.

While the chain structure of **1** was expected, the zigzag feature of the chain was a surprise. Indeed, the other two regular Mn^{II}-Cu^{II} chain compounds described so far, $MnCu(pba)(H_2O)_3 \cdot 2H_2O$ and $MnCu(pbaOH)(H_2O)_3$, present a ribbonlike structure with a *trans* coordination of the water molecules in the manganese coordination sphere.[19,29]

The bimetallic chains in **1** are almost perfectly isolated from each other. The intrachain interaction between nearest neighbor ions is rather large ($J_{MnCu} = -31.3$ cm^{-1}), but the interchain interactions are negligibly small. To obtain a compound behaving as a magnet, in a single trial, we attempted to bring the chains closer to each other by selectively removing the apical ligand weakly bound to copper. The technique employed proved successful in the case of $MnCu(pbaOH)(H_2O)_3$. As a matter of fact, this compound behaves as a magnet below $T_c = 4.6$ K; when the water molecule in the copper coordination sphere is removed, T_c is shifted up to 30 K.[20] For **1**, the thermal treatment we needed to apply was more severe, and we did not succeed in removing only one among three DMSO molecules. Warming **1** at 140 °C under vacuum afforded an amorphous material, **2**. The chemical analysis is compatible with 0.7 DMSO molecule per MnCu(opba) unit. Perhaps some bonds are created between the manganese atom of a chain and the oxamato oxygen atoms of an adjacent chain. The chains are now disordered and possibly broken into smaller fragments. The magnetic properties of **2** are rather peculiar. The $M = f(T)$ curves reveal a magnetic transition at $T_c = 6.5$ K with a spontaneous magnetization below T_c. The magnetic transition, however, is less abrupt than for the other $Mn^{II}Cu^{II}$ molecular-based magnets. It is, in particular, much less abrupt than for **3** and **4** (vide infra). The $M = f(T)$ curve at 2 K, i.e. in the magnetically ordered phase, displays the expected high zero-field susceptibility, $(\partial M/\partial H)_{H=0}$, and then a saturation which is only half of that observed for the precursor **1**. This behavior is probably related to the amorphous character of the material. The structural disorder can create some Mn(II)–Mn(II) and Cu(II)–Cu(II) antiferromagnetic interactions in addition to the dominant Mn(II)–Cu(II) interactions. It can also favor noncollinear local anisotropy directions. At this stage, it is probably worth mentioning that the magnetic behavior of **2** is perfectly reproducible in different samples arising from different preparations. Recently, in a very stimulating talk and paper, Palacio emphasized that the ferromagnetism in disordered phases might well be one of the interesting new phenomena in molecular magnetism.[34] It is remarkable that our compound **2** presents most of the features postulated by Palacio for this kind of disordered magnet.

We stated at the beginning of this section that the zigzag structure of the chains in **1** was a surprise. Actually, it was a surprise that stimulated new experiments. Indeed, this zigzag character results from the *cis* coordination of the DMSO molecules

(33) Bencini, A.; Gatteschi, D. *EPR of Exchange Coupled Systems*; Springer-Verlag: Berlin, 1990.
(34) Palacio, F. In ref 4.

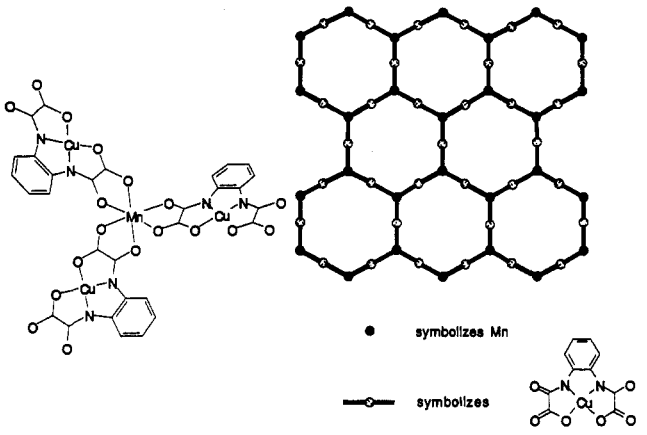

Figure 10. Postulated structure for the $Mn_2[Cu(opba)]_3$ skeleton in $(NBu_4)_2Mn_2[Cu(opba)]_3 \cdot 6DMSO \cdot H_2O$ (3) and $(NBu_4)_2Mn_2[Cu(opba)]_3$ (4): left, environment of a manganese atom; right, $Mn_2[Cu(opba)]_3$ two-dimensional network.

around manganese, and this *cis* coordination suggests that it should be possible to replace these two DMSO molecules by a bisbidentate ligand like $[Cu(opba)]^{2-}$ and so to cross-link the chains and increase the dimensionality of the system. This idea led us to the compounds **3** and **4** behaving as magnets below 15 and 22 K, respectively. The problem we are faced with is determining the crystal structures of **3** and **4**. The same problem was recently encountered by Okawa and co-workers with their mixed-metal ferro- or ferrimagnetic assemblies[22] of formula $(NBu_4)[MCr(ox)_3]$. In our case, we had already obtained nicely shaped single crystals of **3**, but they were still too small. Furthermore, the six DMSO molecules within the lattice as well as the NBu_4^+ organic cations might be disordered, which makes even more complicated the refinement of the structure. Although we have already spent much time trying to obtain single crystals of **3** suitable for a structure determination, the situation is certainly not hopeless.

The possible structure of **3** may be conceived by considering the crystal structures of several compounds with the $M_2[Cu(pba)]_3$ stoichiometry.[35-37] In these compounds, M is a trivalent rare earth metal ion instead of a divalent 3d ion and pba is 1,3-propanediylbis(oxamato). In all the cases, M is surrounded by three Cu(pba) moieties. Similarly, the manganese atom in **3** is most likely surrounded by three Cu(opba) groups instead of two in the chain compounds like **1**. The manganese atom is expected to retain its octahedral environment. Therefore, the three copper atoms surrounding it should occupy the three corners of an equilateral triangle, the center of which is occupied by the manganese atom. The Mn–Cu directions then would be directed at 120° angles to each other, as schematized in Figure 10 (left). We can note that a $Mn^{II}Cu^{II}_3$ cluster with this type of environment for the central manganese atom has already been described.[38] The simplest structure respecting the $Mn_2[Cu(opba)]_3$ stoichiometry, in which the manganese atom is surrounded as in Figure 10 (left), is schematized in Figure 10 (right). This structure may also be described as a two-dimensional honeycomb network of edge-sharing hexagons. It is reminiscent of that of $M_2(ox)_3 \cdot 9.5H_2O$ with M = La or Gd, replacing Mn, and ox = oxalato, replacing Cu(opba).[39,40] Our description is obviously somewhat idealized. In particular, it ignores the presence of an apical DMSO molecule in the copper coordination sphere. The square pyramidal environment of the copper atom in **3** is unambiguously demonstrated by the frequency of the copper $^2B_1 \rightarrow {}^2A_1$ transition at 590 nm.[41] Moreover, our structural model specifies the positions neither of the noncoordinated DMSO molecules nor of the $(NBu_4)^+$ cations. More complicated structures, although less probable, may not be completely ruled out. The important point is that the magnetic properties of **3** are consistent with such a two-dimensional structure. Let us justify this statement. In an ideal $Mn^{II}Cu^{II}$ magnetic lattice with three interaction parameters, J_x, J_y, and J_z, the critical temperature T_c is roughly proportional to $(J_xJ_yJ_z)^{1/3}$. In **1**, one of the interaction parameters is equal to -31.3 cm^{-1} while the other two are close to zero; T_c is too low to be detected. If J_x, J_y, and J_z were of the same order of magnitude, around -31 cm^{-1}, T_c would be expected to be very high, perhaps close to 200 K. In **3**, T_c is equal to 15 K, which strongly suggests that one of the interaction parameters remains small. In other terms, along one of the directions the interactions would be through space instead of through bond, which is consistent with a two-dimensional structure. In **4**, the planes consisting of edge-sharing hexagons should be slightly closer to each other, which results in an increase of T_c.

Conclusion

The first molecular magnets which were described all had a one-dimensional structure. The low values of the critical temperatures were due to the fact that, whatever the magnitude of the intrachain interaction, the interchain interactions were very weak. To improve the performances of these molecular materials, it was necessary to increase the dimensionality. Before this work, we explored two pathways along this line. The first was to bring the chains closer to each other by removing selectively some apical ligands, which led us to a compound ordering at 30 K.[20] The second was to use Cu(II) units such as

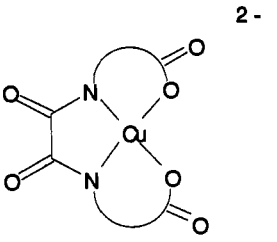

whose carboxylic functions could bind to the manganese(II) ion of another unit, affording a two- or three-dimensional network, which led to a compound ordering at 14 K.[21,42] Neither of these two approaches was perfectly controlled from a synthesis point of view, and we must recognize that serendipity also helped us. For instance, the thermal treatment removing selectively the water molecule in the copper coordination sphere of $MnCu(pbaOH)(H_2O)_3$ could have modified the relative positions of the chains in the lattice and favored antiferromagnetic instead of ferromagnetic interchain interactions. Fortunately, this was not the case.

In this paper, in contrast, we attempted to construct a two-dimensional network in a more controlled fashion. The *cis* coordination around the manganese atom in **1** suggests that two DMSO molecules could be replaced by another Cu(opba) group which would cross-link the chains in a two-dimensional network. Such a situation seems to be achieved in **3** and **4**. We have not been able to grow single crystals sufficiently large for a structural determination. However, the magnetic properties agree with such a two-dimensional character. While the chain compound **1** does not show any indication of long-range ordering, **3** and **4** exhibit

(35) Guillou, O.; Bergerat, P.; Kahn, O.; Boubekeur, K.; Batail, P. *Inorg. Chem.* **1991**, *31*, 110.
(36) Guillou, O.; Oushoorn, R. L.; Kahn, O.; Boubekeur, K.; Batail, P. *Angew. Chem., Int. Ed. Engl.* **1992**, *31*, 626.
(37) Guillou, O.; Kahn, O.; Oushoorn, R. L.; Boubekeur, K.; Batail, P. *Inorg. Chim. Acta* **1992**, *198*, 119.
(38) Lloret, F.; Journaux, Y.; Julve, M. *Inorg. Chem.* **1990**, *29*, 3967.
(39) Ollendorf, W.; Weigel, F. *Inorg. Nucl. Chem. Lett.* **1969**, *5*, 263.
(40) Michaelides, A.; Skoulika, S.; Aubry, A. *Mater. Res. Bull.* **1988**, *23*, 579.
(41) Nakatani, K.; Kahn, O.; Mathonière, C.; Pei, Y.; Zakine, C. *New J. Chem.* **1990**, *14*, 861.
(42) Lloret, F.; Julve, M.; Ruiz, R.; Journaux, Y.; Nakatani, K.; Kahn, O.; Sletten, J. *Inorg. Chem.* **1993**, *32*, 27.

abrupt magnetic transitions at T_c = 15 and 22 K, respectively, with first-magnetization curves below T_c characteristic of almost ideal magnets. In the magnetically ordered phase, the S_{Mn} and S_{Cu} local spins are aligned opposite to each other.

The mechanism of the dominant Mn(II)–Cu(II) interactions through the oxamido bridge is rather well understood; these interactions are due to the overlap of the $d_{x^2-y^2}$ magnetic orbitals centered on adjacent spin carriers. On the other hand, the nature of the through-space interactions, without which there would be no long-range ordering, is still obscure. In the very near future, we will report new structural and magnetic data providing some important information concerning this question.

Supplementary Material Available: Listings of experimental crystallographic data, coordinates and isotropic displacement parameters, anisotropic thermal parameters, distances and angles involving hydrogen atoms, and least-squares planes (Tables SI–SVI) (8 pages); a table of calculated and observed structure factors (17 pages). Ordering information is given on any current masthead page.